Hydrology Research

Hydrology Research Vol 54 No 4, 451 doi: 10.2166/nh.2023.081

Application of Benfratello's method to estimate the spatio-temporal variability of the irrigation deficit in a Mediterranean semiarid climate

Marco Peli *, Cesare Rapuzzi, Stefano Barontini and Roberto Ranzi

Dipartimento di Ingegneria Civile, Architettura, Territorio, Ambiente e di Matematica (DICATAM), Università degli Studi di Brescia, via Branze 43, Brescia 25123, Italy

*Corresponding author. E-mail: marco.peli@unibs.it

MP, 0000-0003-3481-2296

ABSTRACT

This work presents a novel, spatially distributed, GIS-based application of Benfratello's conceptual method (developed in the 1960s) to estimate the climatic water deficit and the irrigation deficit at the field and basin scales. Explicit analytical relationships are obtained to define the deficit uncertainty on the basis of the interannual variability of temperature and precipitation. With this model, we aim at proposing a rather simple and effective tool to deal with the complicated issues of assessing the soil water balance, determining the irrigation deficit and managing the water resources in semiarid agricultural environments, in the context of climatic, land-use and anthropogenic changes. In order to test this new application, the model was applied to estimate the irrigation deficit of the Bonifica della Capitanata consortium in the Apulia region, one of the most important agricultural districts in Southern Italy and in the whole Mediterranean area, in four different historical land-use scenarios. The first results of the application seem encouraging, as by using a limited amount of parameters we estimated an irrigation demand which is in agreement with the irrigation volumes supplied by the consortium. The different land-use cases are discussed in the light of an application of the Budyko curve.

Key words: Capitanata agricultural district, climate change adaptation, climatic water deficit, crop water requirement, wadi hydrology, water balance

HIGHLIGHTS

- We present a GIS-based implementation of Benfratello's method to assess the climatic water deficit and the irrigation water deficit.
- Explicit relationships are proposed to initialize the method and to determine the variability of the annual deficit.
- Starting from the Budyko curve, we evaluate the degree of optimization of water resource consumption.
- We apply the method to the Capitanata agricultural district (Southern Italy).

1. INTRODUCTION

In an era of fast climatic evolution as it is the present one, where the hydrological cycle is expected to experience meaningful alterations due to the increased global average air temperature, agriculture, which is still the main driver of freshwater consumption worldwide (UN-Water 2022) and, at the same time, the main driving sector in poverty reduction and sustainable development (FAO 2021), may face meaningful water shortages. In fact, focusing on the areas surrounding the Mediterranean basin, which are mainly characterized by semiarid and arid conditions, there is high confidence that in future climatic scenarios, the warming will be greater than the world average, and that the increased atmospheric energy and the increased evaporative capacity of the atmosphere will emphasize the hydrological cycle by intensifying the wet season, by increasing the length and severity of droughts and by exposing the soil to more severe dry conditions (Arias *et al.* 2021). Climate scenarios used by Braca *et al.* (2019, 2021) to force a water balance model designed to describe the Italian territory at both national and regional levels depict a meaningful decrease in the groundwater recharge due both to a decrease in precipitation and an increase in air temperature. As an example, they report that the resulting expected decrease in groundwater recharge for the mid-21st century is estimated at about 10 and 17% for the whole Italian territory under scenarios RCP2.6 and RCP4.5, respectively. The expected decrease is greater in Southern regions, e.g. in the Campania region it is predicted at about 13 and

22% under the same scenarios. Analogous results were found by Brussolo *et al.* (2022) for the Piedmont Alpine area considering the present temperature-increasing trend, even if in absence of meaningful precipitation trends.

Irrigation practices often heavily impact both surface and groundwater resources. Therefore the assessment of the consequences on food production and crop yield, of a reduction of water availability, may benefit from simplified water balance models that provide information on the expected irrigation deficit in different climatic and land-use scenarios. With this work, we aim at providing a robust and easy-to-use tool that allows us to make such estimates at the local and district scale. The model is based on a theoretical improvement and on a Geographic Information System (GIS) application of Benfratello's water balance method (Benfratello 1961), originally developed for semiarid and arid agricultural districts in Sicily (Southern Italy), characterized by a Mediterranean climate.

We believe that due to its simplicity, to its elegance and to the small number of needed parameters, Benfratello's method might be regarded as an effective tool to assess the effects of climatic, land-use and anthropogenic change scenarios on the soil water balance and on the irrigation deficit of agricultural crops. In fact, despite the presence, today, of more complex and complete, distributed and semi-distributed hydrological models which well perform at the considered scales (see Xu & Singh 1998; Pereira *et al.* 2020, for a review on this topic), the presented model meets the key need of numerical approaches to find a compromise between the solidity and accuracy characteristics of the solver and the high computational cost associated with the vast spatial and temporal scales typical of environmental problems (Farthing & Ogden 2017). Moreover, as far as in the last decade online water management and irrigation advisory tools have become a widely used resource (Chen *et al.* 2010; Verma *et al.* 2012), the model could fit an application within a webGIS environment, such as a geospatial decision support system to be run in real-time.

From the second half of the 20th century, focusing in particular on the Italian hydrological community, the soil–water balance has been studied both by means of statistical approaches (Viparelli 1956a, 1956b; Quignones 1974; Mantica 1975; Viparelli & Versace 1979) and with conceptually based (Benfratello 1961; Melisenda 1964; Santoro 1991; Casadei *et al.* 1993; Bartolini *et al.* 2011; Braca *et al.* 2019) as well as physically based approaches (Santini 1979, 1992; D'Urso *et al.* 1999; Scalenghe & Ferraris 2009; Romano 2014). In this context, and with a particular focus on agricultural soil, a *classical formulation* (Santoro 1991) was proposed by Benfratello (1961). Benfratello's model is based on a dimensionless form, introduced by De Varennes e Mendonça (1958), of Thornthwaite and Mather's water balance model (Thornthwaite & Mather 1955a, 1955b, 1957). The original Thornthwaite and Mather's model estimates the actual evapotranspiration as a function of Thornthwaite's *potential evapotranspiration* (Thornthwaite 1948), as maximum allowable evapotranspiration – defined as a climatic property – and uses a soil desiccation law that is an exponential function of the potential soil–water loss. The model is still used both for climate characterization (Dourado-Neto *et al.* 2010; Braca *et al.* 2019) and for irrigation deficit assessment (da Silva Tavares *et al.* 2018).

The generalization proposed by Benfratello allows to modulate the soil desiccation law as a power law of the potential soil–water loss, that accounts for the different crop reactions to the water stresses. At its first appearance in 1961, the model was used to estimate the irrigation deficit in Palermo (as representative of a semiarid climate where the field capacity is refilled during the wet season) and in Trapani (as representative of a semiarid climate where the field capacity is not completely refilled during the wet season), both in Sicily. After that, Benfratello (1964) reported about one of the first automatized applications of the model performed by means of the electronic calculator of the Remington Rand center for electronic calculus of the University of Milan, in view of extending the water balance to the whole of Sicily. The method was then used by Melisenda (1965) to explore the variability of the evapotranspiration rate in some representative basins of Sicilian climatology. At the same time Melisenda (1964) proposed a synthetic formulation to immediately calculate the annual irrigation deficit – for the specific case in which Benfratello's method is reduced to Thornthwaite and Mather's one – , based on the definition of a climatic index given by the ratio between the wet-season potential soil–water gain and the dry-season potential soil–water loss. This new formulation was applied to the cases of Catania and Agrigento, as a matching pair of the cases of Palermo and Trapani presented in the 1961 paper.

This methodology was then used by Melisenda (1967b) to define regional climatic maps of Sicily, and it was later made suitable for assessing the monthly irrigation deficit by Santoro (1970) who restored the generality of Benfratello's approach. It is noteworthy that until that time the method was typically applied in view of climatic analyses and by performing the calculations at a monthly scale. In this sense, it is coherent with the purposes of the use of Thornthwaite's method to assess the maximum evapotranspiration as a climatic factor that is not directly related to the crop. In the same direction, in another work by Benfratello *et al.* (1979), the method was used as an indirect procedure to estimate the groundwater

recharge for the Sicilian aquifers. On the other hand, Melisenda (1967a) applied the method, still in Thornthwaite and Mather's simplified form, to design the irrigation schedule at a weekly scale and applied it to the case of Lentini agricultural lands. Later, the model was applied to assess the water balance also in other climatic conditions, both in Italy (Casadei *et al.* 1993) and abroad (Dumitru *et al.* 2009).

In this work, we come back to the original Benfratello's model and we propose a theoretical development that allows (*a*) to explicitly initialize the model for two cases of Benfratello's desiccation power law and (*b*) to explicitly determine the deficit uncertainty on the basis of the knowledge of the interannual variability of temperature and precipitation.

We propose a GIS-based implementation of the model (with QGIS 3.10 and custom Python scripts) and we present an application to the study of the case of the Capitanata district (Apulia, Southern Italy), which is one of the main agricultural districts in the Mediterranean basin (see, e.g. Lamaddalena *et al.* 2004, 2008; Portoghese *et al.* 2005; Guyennon *et al.* 2016, 2017; de Vito *et al.* 2019; Dragonetti *et al.* 2020). The model was applied to determine both the climatic water deficit, i.e. by estimating the maximum required evapotranspiration as Thornthwaite's potential evapotranspiration, and the agricultural water deficit, i.e. by estimating the maximum required evapotranspiration by means of Hargreaves' method modulated with the FAO procedure (Allen *et al.* 1998), in four different land-use conditions provided by the Apulia administrative authority.

In the following, after recalling the original structure of Benfratello's water balance method and presenting our theoretical development (Section 2), we introduce the Capitanata case study (Section 3) and the GIS-based application of the model (Section 4). In the Discussion (Section 5), we present the potentialities of this application also on the basis of the classical Budyko (1974) curve and of an irrigation-deficit curve obtained by transforming the Budyko one.

2. BENFRATELLO'S ESTIMATE OF IRRIGATION DEFICIT

2.1. Original estimate of the expected deficit

2.1.1. Problem statement

In the following, we will present Benfratello's method as it was first introduced in 1961 (see Figure 1 for a sketch of the control volume). According to the original hypotheses, there is no water capillary rise from the groundwater table to the soil, and runoff and percolation take place only after the soil water reached the field capacity (U). The simplified soil water balance of the ith month and of the jth year is therefore given by:

$$\Delta A_{i,j} = P_{i,j} - ET_{i,j} - S_{i,j} \tag{1}$$

where $A_{i,j} \leq U[L]$ is the equivalent depth of the available stored water at the end of the month, $\Delta A_{i,j} = A_{i,j} - A_{i-1,j}$ is the variation of the available water, $P_{i,j}[L]$ is the monthly precipitation, $ET_{i,j}[L]$ is the monthly (actual) evapotranspiration and $S_{i,j}[L]$ is the cumulated water exceedance, i.e. the summation of runoff and percolation. The usage of the letters D and S, standing for the Latin words *deficit* (*it lacks*) and *superavit* (*it exceeded*), was early introduced by De Varennes e Mendonça (1958) and later maintained by Benfratello (1961).

The monthly deficit $D_{i,j}$ is calculated as the amount of water needed to fill the gap between the maximum required evapotranspiration $ET_{\max,i,j}$ and the actual one $ET_{i,j}$. It is worth recalling that the definition of Thornthwaite's potential evapotranspiration, and the values calculated by means of Thornthwaite's formula, have a climatic meaning and they are not considered by the FAO procedure in order to estimate the maximum required evapotranspiration for irrigation purposes (Allen *et al.* 1998). According to this procedure, in fact, the maximum required evapotranspiration $ET_{\max,i,j}$ is estimated by modulating the reference crop evapotranspiration with coefficients that account for the considered crop and for its phenological development. The reference crop evapotranspiration is in turn estimated by means of Penman–Monteith's formula (as in, e.g., Licciardello *et al.*, 2011), or in case of scarce data, by means of Hargreaves' formula. In this paper, $ET_{\max}$ was calculated both with Thornthwaite's formula and with FAO procedure, in order to explore the possibility of using the method to assess both the climatic water deficit and the irrigation water demand.

The calculations are performed on a climatic basis, which means that taking the expectation of the water balance, the method provides the expectation of the monthly deficit. Therefore, once defined the expectations of $A_{i,j}$, $P_{i,j}$, $ET_{i,j}$, $S_{i,j}$ and

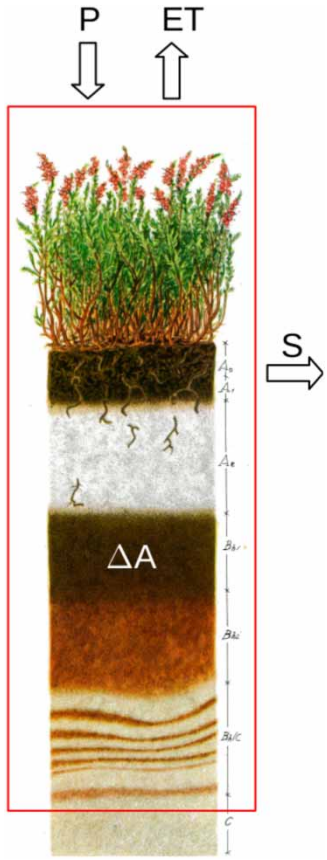

Figure 1 | Control volume of Benfratello's water balance sketched on the soil n.1 of Plate 22 by Kubiena (Humus podsol). Symbols meaning is explained in the text.

$D_{i,j}$, as A_i, P_i, ET_i, S_i, and D_i, respectively, the water balance and the irrigation deficit are rewritten as:

$$\Delta A_i = P_i - ET_i - S_i \tag{2}$$

$$D_i = ET_{\max,i} - ET_i \tag{3}$$

In the original method $ET_{\max,i}$ was a climatic factor, estimated as Thornthwaite's potential evapotranspiration (Thornthwaite 1948). The method is anyway flexible and the maximum required evapotranspiration may alternatively be estimated as the maximum evapotranspiration of a specific crop according, e.g., to the consolidated FAO procedure.

In order to perform the calculations, Benfratello divided the year into a dry season and into a wet season, on the basis of a comparison between the monthly precipitation P_i and the monthly maximum required evapotranspiration $ET_{\max,i}$. This is possible for climates having one major rainfall season, as the Mediterranean one is. The dry season starts when:

$$P_i < ET_{\max,i} \tag{4}$$

and ends when:

$$P_i \geq ET_{\max,i} \tag{5}$$

It is assumed that during the wet season:

$$ET_i = ET_{\max,i} \tag{6}$$

and all the precipitation excess firstly refills the deficit with respect to field capacity and only when the latter is reached, runoff and groundwater recharge are generated. Therefore, during the wet season, the water balance is fully defined as:

$$\Delta A_i + S_i \quad = P_i - ET_{\max,i} \tag{7}$$

$$S_i > 0 \quad \text{when } A_i = U \tag{8}$$

During the dry season instead, the water exceedance S_i is null, because the evapotranspiration demand is greater than the precipitation, and the soil water partially compensates for it. It is therefore not possible that the field capacity is reached during the dry season, a part that at its beginning, and the soil water balance is rewritten as:

$$\Delta A_i = P_i - ET_i \tag{9}$$

2.1.2. Derivation of the desiccation law

Let us fix the origin of the time axis $t = 0$ at the beginning of the dry season. The dry-season water balance is then fully defined once it is possible to determine one between the actual evapotranspiration $ET(t)$ and the desiccation law of the soil $A(t)$. In order to do so, Benfratello rewrote the water balance in terms of cumulated values from the beginning of the dry season $t = 0$:

$$A(t) - A_{\max} = P(t) - ET(t) \tag{10}$$

where $A_{\max}$ is the maximum soil water content, reached at $t = 0$. It may be $A_{\max} \leq U$ depending on the local climate, as it is defined later. In Equation (10), $P(t)$ and $ET(t)$ are the cumulated precipitation and evapotranspiration at a certain instant t. With the symbols of the 1961 paper, the potential soil water loss $-L(t)$ (with $L(t)$ intrinsically negative) and the actual soil water loss $B(t)$ are introduced as:

$$-L(t) = ET_{\max}(t) - P(t) \tag{11}$$

$$B(t) = ET(t) - P(t) \tag{12}$$

The fundamental hypothesis of the method, needed to link the soil desiccation law to the actual evapotranspiration, is now introduced:

$$\frac{\mathrm{d}B/\mathrm{d}t}{-(\mathrm{d}L/\mathrm{d}t)} = \left(\frac{A}{U}\right)^m \tag{13}$$

This law expresses the concept that the ratio of the actual to the potential water losses is proportional to the ratio of soil water content to field capacity. According to Equation (13) the ratio between the actual and the potential rates of soil water loss is a power function of the available soil water normalized with the field capacity. According to the water balance of the dry season (Equation (10)) $\mathrm{d}B = -\mathrm{d}A$, so that Equation (13) is simplified as:

$$\frac{\mathrm{d}A}{\mathrm{d}L} = \left(\frac{A}{U}\right)^m \tag{14}$$

The power $m \geq 0$ accounts for the different attitudes of the crop to react to water stress and it generalizes the Thornthwaite and Mather's approach in which $m = 1$.

Following De Varennes e Mendonça (1958), the dimensionless variables $\alpha(t)$ and $\lambda(t)$ were introduced:

$$\alpha(t) = \frac{A(t)}{U} \tag{15}$$

$$\lambda(t) = \frac{L(t)}{U} \tag{16}$$

Equation (14) is rewritten as:

$$\frac{d\alpha}{d\lambda} = \alpha^m \tag{17}$$

with the initial condition:

$$\alpha(0) = \alpha_{max} \tag{18}$$

where $\alpha_{max} = A_{max}/U(\leq 1)$. In Figure 2 (left), Equation (17) is plotted for different values of m and for $\alpha_{max} = 1$. In case $m > 1$ the crop reacts to water stress by strongly reducing its transpirative capacity, on the contrary, if $m < 1$ the crop reacts by only weakly reducing it. The limit case $m = 0$ means that the crop does not react to the water shortage and always tries to satisfy the maximum transpirative demand.

The solution of Equation (17) with the condition (18) provides the (normalized) desiccation law of the soil $\alpha(\lambda)$ as a function of the cumulated and normalized potential soil–water loss, which is a known function of the climate and of the crop. Four cases, as reported in Table 1, are usually given for the solution, depending on $\alpha_{max} = 1$ or $\alpha_{max} < 1$ and for $m = 1$ or $m \neq 1$. In Figure 2 (right) some solutions of Equation (17) are plotted for different values of m and for $\alpha_{max} = 1$. It is worth noting that for $m < 1$ the soil completely dries out for finite values of the potential soil–water loss $-\lambda$, while for $m = 1$ the soil only asymptotically dries out.

2.1.3. Model initialization

In order to apply the method a procedure is now needed to determine whether α_{max} is ≤ 1. Let us define the soil water gain during the wet season Σ_w, and its dimensionless form σ_w, as it was previously defined L:

$$\Sigma_{w,i} = P_i - ET_{max,i} > 0 \tag{19}$$

$$\sigma_{w,i} = \frac{\Sigma_{w,i}}{U} \tag{20}$$

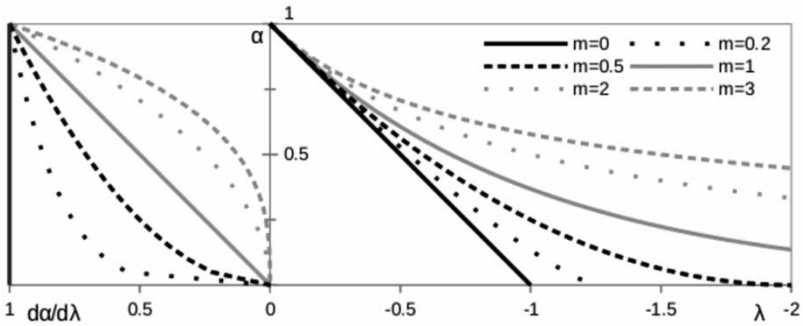

Figure 2 | Fundamental laws of Benfratello's method. Left: evapotranspiration law $d\alpha/d\lambda$ as given by Equation (17). Right: desiccation law $\alpha(\lambda)$ as given in Table 1.

Table 1 | Solutions of Equation (17) with the condition (18), for different cases of α_{max} and m. The meaning of the symbols is reported in the text

	$m = 1$	$m \neq 1$
$\alpha_{max} = 1$	$\alpha = e^{\lambda}$	$\alpha = [1 + (1-m)\lambda]^{1/(1-m)}$
$\alpha_{max} < 1$	$\frac{\alpha}{\alpha_{max}} = e^{\lambda}$	$\frac{\alpha}{\alpha_{max}} = \left[1 + (1-m)\frac{\lambda}{\alpha_{max}^{1-m}}\right]^{1/(1-m)}$

Let us define $-\lambda_{\min}$, $\alpha_{\min}$ and $\sigma_{w,\max}$ as the dimensionless forms of the maximum potential loss during the dry season, of the minimum available soil water at the end of the dry season, and of the maximum soil water gain at the end of the wet season, respectively. In case $\alpha_{\max} < 1$, i.e. the precipitation surplus during the wet season is not enough to refill the soil field capacity, the annual water balance is written as:

$$\alpha_{\min} = \alpha(\lambda_{\min}) \tag{21}$$

$$\alpha_{\max} = \alpha_{\min} + \sigma_{w,\max}, \tag{22}$$

where Equation (21) stands for the dry season and Equation (22) stands for the wet season. From Equations (21) and (22), $\alpha_{\max}$ and $\alpha_{\min}$ are determined. In case the computed value of $\alpha_{\max} > 1$, it is a signal that $\alpha_{\max}$ should be posed equal to 1, since the precipitation surplus is effective at refilling the field capacity, and the water exceedance will accordingly emerge from the water balance of Equations (7) and (8).

The system given by Equations (21) and (22) is analytically solvable in some cases as e.g. those for $m = 0.5$, $m = 1$ and $m = 2$. The solutions are provided in Table 2.

2.1.4. Deficit estimate

The expectation of the annual deficit D is given by the summation of the monthly deficit D_i given by Equation (3), over the whole dry season. Having defined t_w the time at which the wet season begins, with the same convention introduced for Equation (10), the cumulated irrigation deficit at the end of the dry season is given by:

$$D(t_w) = ET_{\max}(t_w) - ET(t_w) \tag{23}$$

According to Equations (11) and (12), and accounting for the simplified water balance of Equation (10), we can write:

$$D(t_w) = -L(t_w) - B(t_w) \tag{24}$$

$$D(t_w) = -L(t_w) + A_{\min} - A_{\max} \tag{25}$$

where $A_{\min}$ and $A_{\max}$ are the available soil water at the end and at the beginning of the dry season, respectively. In the dimensionless form we obtain:

$$\delta(t_w) = -\lambda_{\min} + \alpha_{\min} - \alpha_{\max}, \tag{26}$$

where $\delta = D/U$ is the dimensionless deficit.

2.1.5. Method application

The method is traditionally applied as follows:

1. The field capacity U and the power m are chosen.
2. The value of $\alpha_{\max}$ is calculated on the basis of the system of Equations (21) and (22), or with the solutions of Table 2.
3. Starting from the beginning of the dry season, the cumulated value of $L(t)$ given by Equation (11) and of the corresponding dimensionless form $\lambda(t)$ is calculated at the end of each month of the dry season.

Table 2 | Values of $\alpha_{\max}$ for different values of m

$m = 0.5$	$m = 1$	$m = 2$
$\alpha_{\max} = \left(\frac{\sigma_{\max}}{-\lambda_{\min}} - \frac{\lambda_{\min}}{4}\right)$	$\alpha_{\max} = \frac{\sigma_{\max}}{1 - e^{\lambda_{\min}}}$	$\alpha_{\max} = \frac{\sigma_{\max}}{2}\left(1 + \sqrt{1 - \frac{4}{\sigma_{\max}\lambda_{\min}}}\right)$

4. The values of $\alpha(\lambda)$ are determined at the same times, with the solutions reported in Table 1, and consequently the values of the available water A_i at the end of each ith month of the dry season are calculated.
5. The actual evapotranspiration ET_i is determined via the water balance of Equation (9).
6. From the end of the dry season, i.e. for the whole wet season, the water balance of Equations (7) and (8) hold and allow us to determine the soil water refill ΔA_i and the water exceedance S_i for each month.
7. At the end of the wet season, the initial state of the soil $A_{\max}$ is restored.
8. The monthly irrigation deficit D_i is calculated during the dry season at the end of each month by means of Equation (3).
9. The yearly irrigation deficit D is finally calculated by means of Equations (24) and (25).

As an example of Benfratello's method application at the field scale, Figure 3 shows the water balance components in Foggia, determined with $U = 300$mm, $A_{\max} = 64$mm, $m = 0.5,\ 1,\ 2$, paired with the local climograph for the period 1950–2007 to show the precipitation and temperature regimes.

2.2. Proposal of an estimate of the deficit uncertainty

The traditional application of Benfratello's method is meant to provide an estimate of the expectations of the monthly and annual components of the water balance in a semiarid climate. Though the climate shows interannual variability, so that, in order to use the obtained results as design input for irrigation purposes, it is relevant to determine also the uncertainty of the irrigation deficit, as a consequence of the interannual variability of the climatic variables, viz temperature and precipitation. In the following lines, we will present an improvement of Benfratello's method to do so.

As a first step, we need to define the interannual variability of L and Σ_w. According to the method, in fact, all the climatic variability affects the monthly values of L_i and $\Sigma_{w,i}$. For each ith month during the dry or the wet season, respectively, the variabilities $\sigma(L_i)$ and $\sigma(\Sigma_{w,i})$ are given as a function of the interannual standard deviations of the maximum required evapotranspiration $\sigma(ET_{\max,i})$ and of the precipitation $\sigma(P_i)$. Assuming the independence of the maximum evapotranspiration

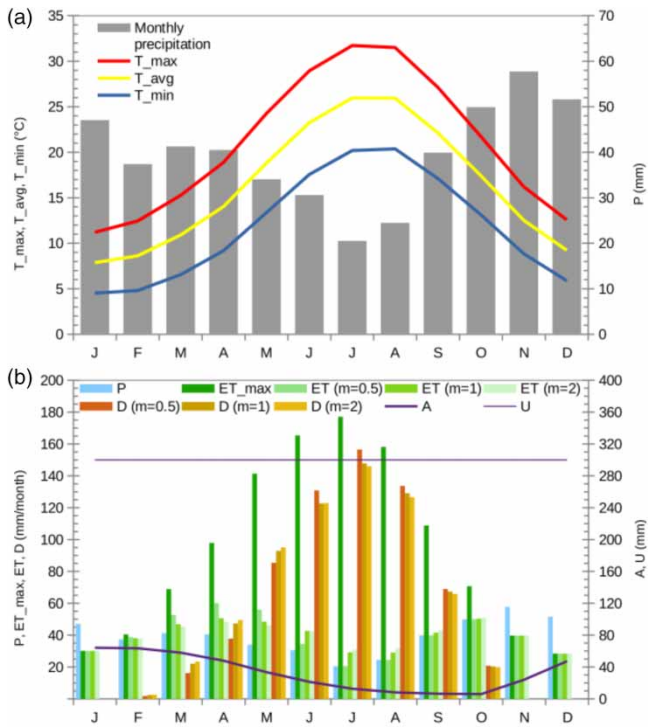

Figure 3 | (a) Climograph of Foggia (1950–2007) and (b) water balance components in Foggia, according to Benfratello's method with $U = 300$ mm, $A_{\max} = 64$ mm, $m = 0.5, 1, 2$.

$ET_{\max,i}$ and of the precipitation P_i, the variabilities $\sigma(L_i)$ and $\sigma(\Sigma_{w,i})$ are given by:

$$\begin{aligned}\sigma(L_i) &= \sqrt{\sigma^2(ET_{\max,i}) + \sigma^2(P_i)}, \quad i \in \text{ dry season},\\ \sigma(\Sigma_{w,i}) &= \sqrt{\sigma^2(ET_{\max,i}) + \sigma^2(P_i)}, \quad i \in \text{ wet season}.\end{aligned}$$

If $ET_{\max,i}$ basically depends on the monthly temperature T_i, the previous relationships are rewritten in the form:

$$\sigma(L_i) = \sqrt{\left(\frac{\mathrm{d}ET_{\max}}{\mathrm{d}T}\right)^2\Big|_{T=T_i}\sigma^2(T_i) + \sigma^2(P_i)}, \quad i \in \text{ dry season}, \tag{27}$$

$$\sigma(\Sigma_{w,i}) = \sqrt{\left(\frac{\mathrm{d}ET_{\max}}{\mathrm{d}T}\right)^2\Big|_{T=T_i}\sigma^2(T_i) + \sigma^2(P_i)}, \quad i \in \text{ wet season}, \tag{28}$$

In dimensionless form we obtain:

$$\sigma(\lambda_i) = \frac{\sigma(L_i)}{U}, \tag{29}$$

$$\sigma(\sigma_{w,i}) = \frac{\sigma(\Sigma_{w,i})}{U}. \tag{30}$$

From Equations (27) and (28), or alternatively from Equations (29) and (30), the annual values of $\sigma(L)$ and $\sigma(\Sigma_w)$ might be calculated with the following form:

$$\sigma(L) = \sqrt{\Sigma_i \sigma^2(L_i)}, \quad i \in \text{ dry season} \tag{31}$$

$$\sigma(\Sigma_w) = \sqrt{\Sigma_i \sigma^2(\Sigma_{w,i})}, \quad i \in \text{ wet season} \tag{32}$$

As a second step, we define the procedure to determine the deficit uncertainty $\sigma(D)$ on the basis of the interannual variabilities $\sigma(L)$ and $\sigma(\Sigma_w)$. According to the original application of the method the local climate is such that at the end of the wet season, either the soil always reaches the field capacity or the available water is always smaller than the field capacity. In this application, we will not relax this hypothesis in order to determine the deficit uncertainty. Therefore, two cases should be considered, either that at the beginning of the dry season, it is reached or not the field capacity of the soil.

For each jth year, Equation (26) holds in the form:

$$\delta(t_{w,j}) = -\lambda_{\min,j} + \alpha_{\min,j} - \alpha_{\max,j} \tag{33}$$

In the case $A_{\max} < U$ (and $\alpha_{\max} < 1$), by means of Equations (22), Equation (33) takes the form:

$$\delta(t_{w,j}) = -\lambda_{\min,j} + \alpha_{\min,j} - \alpha_{\min,j-1} - \sigma_{w,\max,j-1} \tag{34}$$

By taking the expectation of Equation (34) and assuming that $E[\alpha_{\min,j}] = E[\alpha_{\min,j-1}] = \alpha_{\min}$, we obtain:

$$\delta(t_w) = -\lambda_{\min} - \sigma_{w,\max} \tag{35}$$

In this case, an estimate of the uncertainty $\sigma(\delta(t_w))$ is given by:

$$\sigma(\delta(t_w)) = \sqrt{\sigma^2(\lambda_{\min}) + \sigma^2(\sigma_{w,\max})} \tag{36}$$

and the uncertainty $\sigma(D(t_w))$ is given by:

$$\sigma(D(t_w)) = U\,\sigma(\delta(t_w)) \tag{37}$$

In the case $A_{\max} = U$ ($\alpha_{\max} = 1$), Equations (26) and (33) are rewritten as:

$$\delta(t_w) = -\lambda_{\min} + \alpha_{\min} - 1 \tag{38}$$

$$\delta(t_{w,j}) = -\lambda_{\min,j} + \alpha_{\min,j} - 1 \tag{39}$$

By means of a first-order approximation around $\lambda_{\min}$ and by means of Equation (17), the yearly anomaly $\delta(t_{w,j}) - \delta(t_w)$ is:

$$\delta(t_{w,j}) - \delta(t_w) = -\lambda_{\min,j} + \alpha_{\min,j} - (-\lambda_{\min} + \alpha_{\min}) \tag{40}$$

$$\approx \left(-1 + \frac{\mathrm{d}\alpha}{\mathrm{d}\lambda}\bigg|_{\lambda_{\min}}\right)(\lambda_{\min,j} - \lambda_{\min}) \tag{41}$$

$$= (-1 + \alpha_{\min}^m)(\lambda_{\min,j} - \lambda_{\min}) \tag{42}$$

The uncertainty $\sigma(\delta(t_w))$ is, therefore, given by:

$$\sigma(\delta(t_w)) = \sqrt{(-1 + \alpha_{\min}^m)^2 \sigma^2(\lambda_{\min})} \tag{43}$$

$$\sigma(\delta(t_w)) = |-1 + \alpha_{\min}^m| \sigma(\lambda_{\min}) \tag{44}$$

from which $\sigma(D(t_w))$ is obtained by means of Equation (37).

2.3. GIS application of the method

Traditional applications of Benfratello's method were performed at the local scale, even in the perspective of producing climatic maps. Yet GIS framework allows us to systematically apply it at large scales, accounting for the features of the local climate, soil and cultures. In order to do so, the following (minimal) set of maps is required: soil field capacity, land-use, monthly air temperature and precipitation values with interannual standard deviation as a measure of the interannual variability. The method is applied according to the numbered list presented in paragraph *Method application*.

Finally, the uncertainty of the yearly irrigation deficit $\sigma(D(t_w))$ is locally provided by Equations (36), (44) and by Equation (37).

We now want to define a spatially equivalent estimate of the expectation $D(t_w)$ and of its uncertainty $\sigma(D(t_w))$ over multiple cells of the investigated area. Let $D_{j,k}(t_w)$ be the annual deficit for the jth year and the kth cell and assume that it can be represented by:

$$D_{j,k}(t_w) = D_k(t_w) + z_{j,k}\sigma(D_k(t_w)) \tag{45}$$

where $D_k(t_w)$ and $\sigma(D_k(t_w))$ are the local expectation and uncertainty, respectively, and $z_{j,k}$ is the standard reduced variable corresponding to $D_{j,k}(t_w)$.

If we assume that each realization of temperature and precipitation has the same probability over the whole investigated district, also each $D_{j,k}(t_w)$ has the same probability for each kth cell and the value of $z_{j,k}$ is therefore independent from the cell. Let z_j be this value, so that Equation (45) is written as:

$$D_{j,k}(t_w) = D_k(t_w) + z_j\sigma(D_k(t_w)) \tag{46}$$

and the spatial average $\langle D_{j,k}(t_w)\rangle$ is provided by:

$$\langle D_{j,k}(t_w)\rangle = \langle D_k(t_w)\rangle + z_j\langle\sigma(D_k(t_w))\rangle \tag{47}$$

The equivalent values of the expected deficit and of its uncertainty over the whole area are therefore given by the spatial averages $\langle D_k(t_w)\rangle$ and $\langle\sigma(D_k(t_w))\rangle$, respectively, as they emerge from Equation (47).

2.4. Budyko's framework to highlight the relationship between *ET* and ET_{max}

In the Discussion section, in order to highlight the relationship between ET and ET_{max}, the results will be interpreted in the framework of the classical Budyko curve and of an irrigation-deficit curve obtained by transforming the Budyko curve, for the case of full irrigation. It is therefore worth briefly recalling the shape and the meaning of the two curves.

The Budyko curve (Budyko 1974) puts into relationship the actual annual evapotranspiration, in the form ET/P, with the corresponding maximum annual evapotranspiration ET_{max}/P, the latter being sometimes referred to as Budyko's aridity index. The Budyko curve has the following form:

$$\frac{ET}{P} = \sqrt{\frac{ET_{max}}{P}\tanh\left(\frac{P}{ET_{max}}\right)\left(1-\exp\left(-\frac{ET_{max}}{P}\right)\right)} \tag{48}$$

and its upper bound is the identity line of the first quadrant (i.e. the slope of ET/P for $ET_{max}/P \to 0$) and the asymptote $ET/P = 1$. These two limiting curves represent the cases when ET is maximum, i.e. the case in which ET is energy-limited ($ET/P = ET_{max}/P$) and the case in which ET is water-limited ($ET/P = 1$).

The (climatic) water-deficit curve, in the form D/P, can be straightforwardly obtained by the Budyko curve as:

$$\frac{D}{P} = \frac{ET_{max} - ET}{P}. \tag{49}$$

The irrigation deficit curve is inferiorly bounded by the maximum between $D/P = 0$ and $D/P = (ET_{max}/P) - 1$, which represent the minimum irrigation deficit required, in case the actual evapotranspiration is optimal.

3. THE CAPITANATA CASE STUDY

The investigated area is the Bonifica della Capitanata (the Capitanata reclamation and irrigation district), an area of about 4,410 km^2 in Southern Italy (Apulia region, province of Foggia) which is one of the most important agricultural districts in Italy (Figure 4). The district is Northernly bounded by the Saccione river and Southernly by the Ofanto river. It includes the alluvial plain of the Tavoliere delle Puglie, the second largest plain in Italy with a surface of about 3,000 km^2, mainly cultivated with herbaceous crops, olives, fruit and grapevine trees (Ventrella *et al.* 2012). Part of the Bonifica della Capitanata is irrigated by the following three water-distribution schemes: the major one is the Fortore system in the Northern and Central part, and the others are the Sinistra Ofanto and the Carapelle systems in the Southern part. Particularly, on the Fortore river there is the Occhito reservoir with an active capacity of 250 hm^3, corresponding to about a depth of 210 mm for the total irrigated area. They are on-demand pressurized systems, equipped with water-meters and prepaid card devices for every single user (Lamaddalena *et al.* 2004). According to Lamaddalena *et al.* (2004), the covered area by the consortium distribution network is about 1,404 km^2 and about 90% of it (1,260 km^2) is effectively under-functioning, making the Capitanata one of the greatest and most important irrigation consortia in the Mediterranean region. However the irrigated land is slightly smaller and it is estimated to be about 1,210 km^2 (27.5% of the Bonifica della Capitanata consortium total area), and only 45% of it is irrigated through the consortium water distribution network. In fact, part of the land is directly irrigated by the farmers using private wells and basins as a supplementary or substitutive source.

For the study, monthly maximum and minimum temperature and monthly precipitation of 109 stations located in the Apulia Region, 19 of which fall within the area of interest for the Capitanata consortium, were collected for the period 1950–2007 from the hydrological annals[1].

The Köppen and Geiger climate type of the area, determined according to the procedure suggested by Peel *et al.* (2007), is quite variegated, being in most cases Cfa (Temperate without a dry season and with hot summer), with some Csa (Temperate with dry and hot summer) and a few BSk (Cold arid steppe). In the nearby Promontorio del Gargano (Gargano promontory) there are also some Cfb cases (Temperate without dry season and with warm summer), due to the higher altitude and lower

[1] https://protezionecivile.puglia.it/centro-funzionale-decentrato/rete-di-monitoraggio/annali-e-dati-idrologici-elaborati/annali-idrologici-parte-i/, checked 10 March 2021.

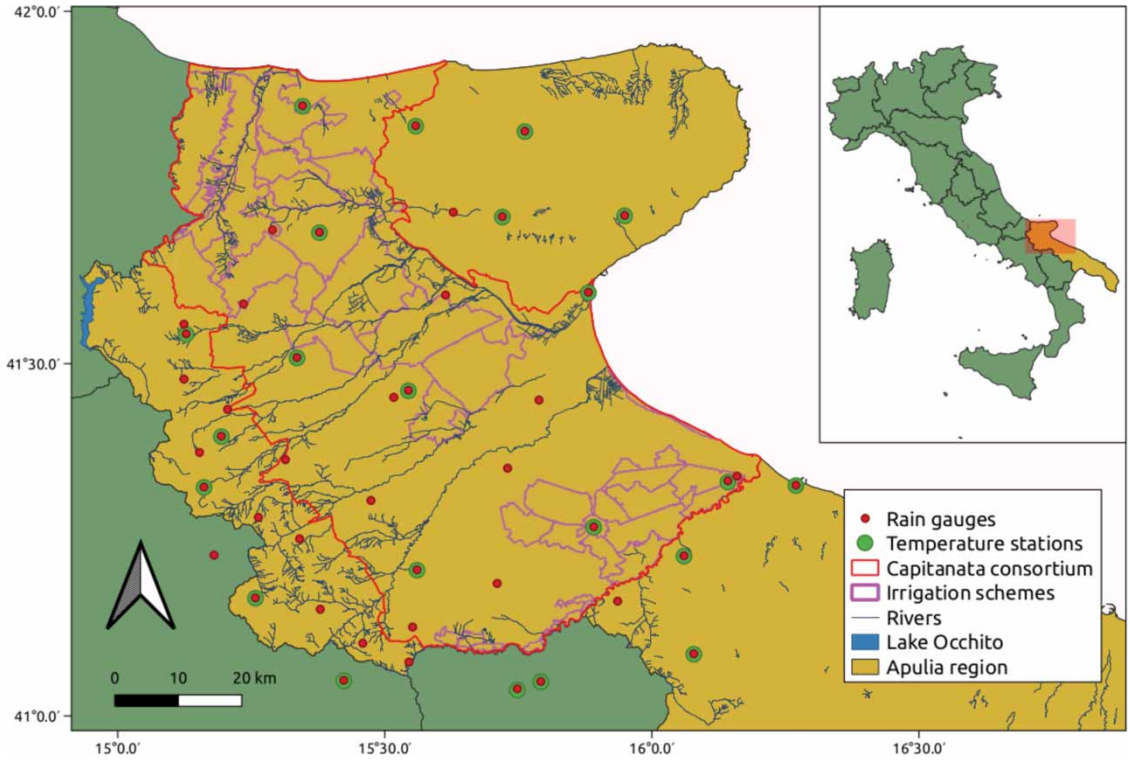

Figure 4 | The Bonifica della Capitanata district in the Northern part of Apulia region, Southern Italy.

temperatures. The precipitation regime is Mediterranean with mostly winter precipitation, which corresponds to the maritimal one among the classification of the Italian pluviometric types by Bandini (1931).

The average annual precipitation in the Capitanata ranges from 400 to 650 mm, and in the surrounding hilly areas it is greater and it reaches 1,160 mm. According to Johansson's continentality index and Kerner's oceanity index, the local climate is maritime but weakly – and mainly in the coastal areas (Lamaddalena *et al.* 2008) – it benefits from the presence of the Adriatic sea. According to both De Martonne's and Pinna-De Martonne's aridity indices the local climate is semiarid (see Baltas 2007, for details on the indices calculation). Finally, the typical summer proneness to water shortages and to droughts in the circum-Mediterranean areas might increase in the near future as stated by Vitale *et al.* (2010) who in recent years observed an increase in the average maximum monthly temperatures (0.35 °C per decade), of the number of tropical nights (4–5 days per decade), of the number of very hot summer days (6 days per decade), and of other indicators that seem to evidence anticipation of the summer dry season. Despite the fact that – as stated by the Authors – these results should be taken with caution because of the relatively short length of the analyzed data series (1979–2008), they are valuable because data were collected in an experimental station located in the Apulian Tavoliere at the centre of the Capitanata.

Also, the effects on groundwater salinity due to the reduced natural discharge from the aquifers are expected to be joined by the impact of the ongoing sea level rise in the Capitanata (Guyennon *et al.* 2017).

4. PRELIMINARY ACTIVITIES

4.1. Input maps preparation

In Table 3, we list the input maps used in order to run Benfratello's method within a GIS framework, which are monthly precipitation, monthly average, maximum and minimum temperature, field capacity and land-cover, needed to modulate the maximum evapotranspiration demand. In order to obtain these maps, we proceeded as follows. Field capacity maps, for different land-cover scenarios, were obtained by multiplying the map of water content at field capacity θ_c by the map of the hydrologically active soil layer. The latter was obtained by assigning a rooted depth to each land-cover class, according to Foxx *et al.* (1984) and Walker (1989). In the nearby Gargano area, despite the deep rooted depth obtained by the referred

Table 3 | Summary of the input layers

Content	Type	Resolution (m)	Ellipsoid and projection	Source
DEM	raster	250	WGS84–UTM32N	INGV
θ_c	raster	250	WGS84–UTM32N	ESDAC
CLC 1990	vector	–	ETRS89–LAEA Europe	GRP
CLC 2000	vector	–	ETRS89–LAEA Europe	ISPRA
CLC 2006	vector	–	ETRS89–LAEA Europe	ISPRA
CLC 2011	vector	–	ETRS89–LAEA Europe	GRP
MS	vector	–	Roma40–Gauss Boaga East	–
P	raster	250	WGS84–UTM32N	–
T, T_{max}, T_{min}	raster	250	WGS 84 UTM 32N	–
U	raster	250	WGS84–UTM32N	–

Note: DEM, Digital Elevation Model; INGV, Istituto Nazionale di Geofisica e Vulcanologia (http://tinitaly.pi.ingv.it); θ_c (cm^3cm^{-3}), Water content at field capacity; ESDAC, European Soil Data Centre (https://esdac.jrc.ec.europa.eu/resource-type/datasets); CLC, Corine Land Cover; GRP, Geoportale Regione Puglia (http://sit.puglia.it); ISPRA, Istituto Superiore per la Protezione e la Ricerca Ambientale (https://www.isprambiente.gov.it/it/attivita/suolo-e-territorio/copertura-del-suolo/corine-land-cover); MS, Meteorological stations location; P(mm), average monthly precipitation; T, T_{max}, T_{min} (^oC), average, maximum and minimum monthly temperature; U(mm), Field capacity.

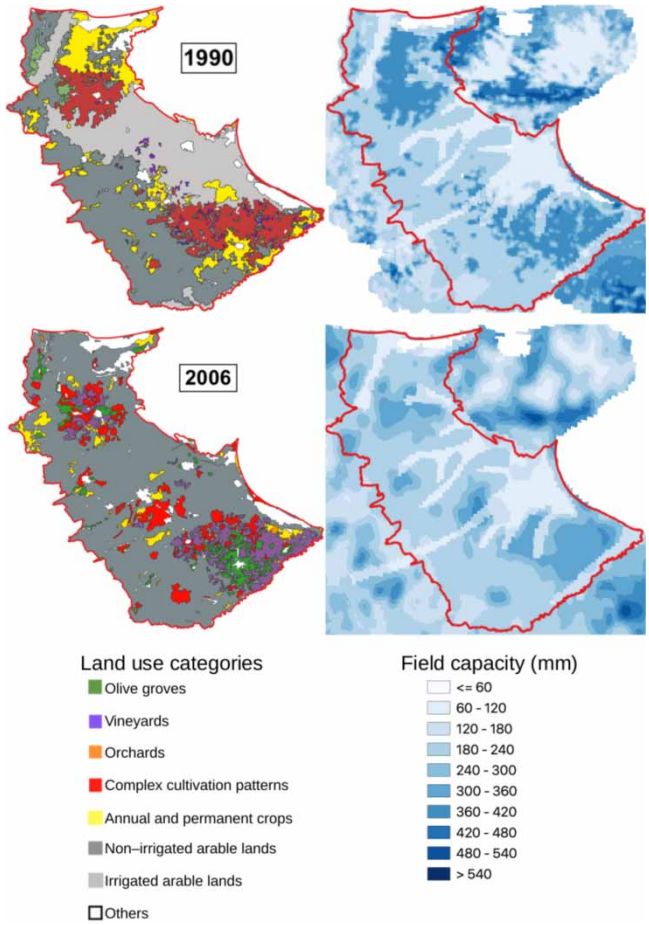

Figure 5 | Maps of the land-cover classification and of the resulting field capacity U of the Bonifica della Capitanata district, according to two different databases made available by the Apulia region administrative authority.

literature, we preferred to assign a shallow hydrologically active soil layer according to Ancona *et al.* (2010) (Figure 5). Monthly precipitation maps were generated from measured precipitation data by means of Thiessen–Voronoi tessellation (see, e.g. Figure 6, top-right map). Monthly temperatures available at the micrometeorological stations were interpolated by a linear function of the elevation in order to provide the temperature maps (see, e.g. Figure 6, top-left map).

4.2. Estimate of the maximum evapotranspiration

The monthly maximum required evapotranspiration was calculated as the crop evapotranspiration in standard conditions according to FAO procedure (Allen *et al.* 1998). In order to do so, the monthly reference evapotranspiration $ET_{\max,o}$ was first calculated by means of Hargreaves' formula:

$$ET_{\max,o} = 0.0023 R_a (T + 17.8) \sqrt{T_{\max} - T_{\min}} \tag{50}$$

where $R_a\,(\mathrm{mm\,d^{-1}})$ is the potentially evaporated water depth corresponding to solar radiation, and it is given as a geographical characteristic, and T, $T_{\max}$, $T_{\min}\,(^{\circ}\mathrm{C})$ are the average, maximum and minimum daily temperatures, respectively. The crop evapotranspiration in standard conditions $ET_{\max}$ was obtained by correcting the former with the cultural coefficients k_c which account for the crop characteristics and for its phenological condition, on a monthly basis. Cultural coefficients were applied according to the tables reported by Allen *et al.* (1998) and updated by Nistor *et al.* (2018) in order to fit the Corine Land Cover classes. As an example, in Figure 6 we present the obtained map of the maximum required evapotranspiration for the month

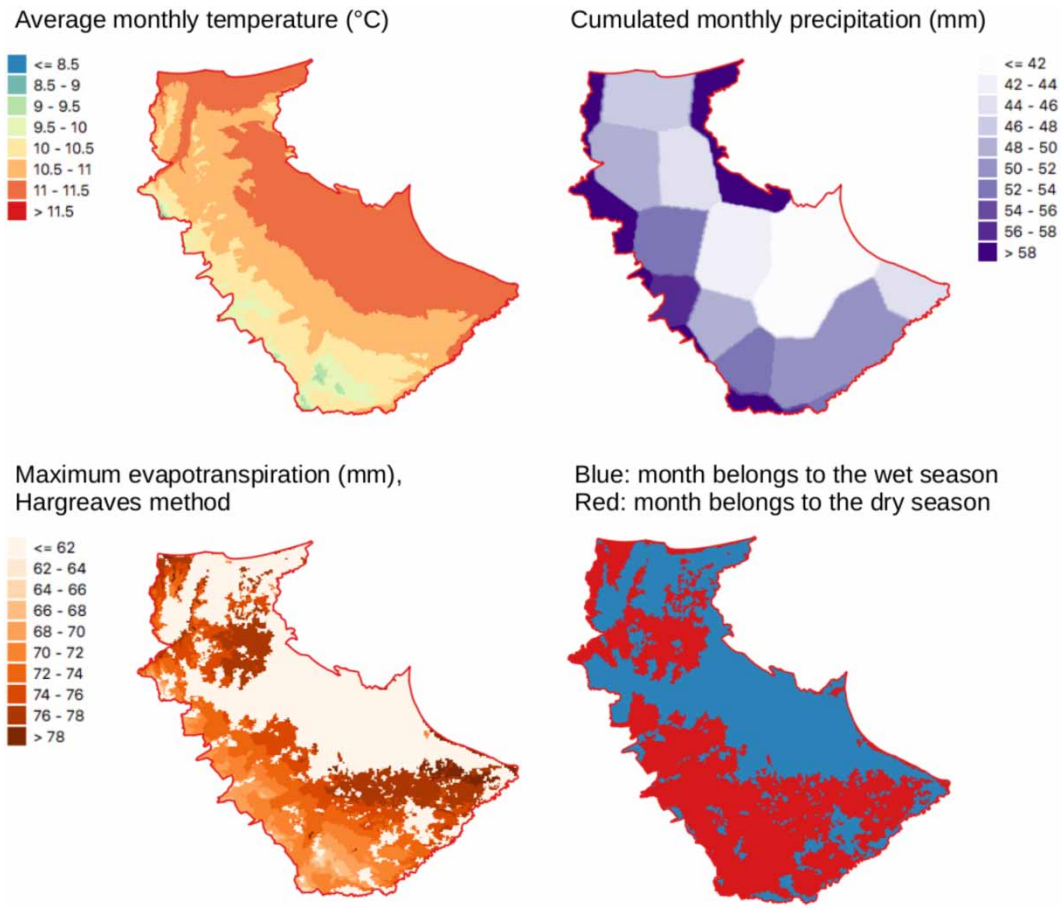

Figure 6 | Maps of the input layers required to run the simulations. As an example, the month of March, at the very beginning of the dry season in some areas of the district, is reported. From top left to bottom right: average monthly temperature T, cumulated monthly precipitation P and maximum evapotranspiration $ET_{\max}$, flag to identify the dry areas, i.e. the areas where $L = P - ET_{\max} < 0$. Please refer to the online version of this paper to see this figure in colour: http://dx.doi.org/10.2166/nh.2023.081.

of March with the 1990 version of the land-cover map (bottom-left map). The application of Benfratello's method largely depends on the beginning of the dry season, therefore it is necessary to assess for each point whether the month is wet or dry depending on the value taken by $L \gtrless 0$. In Figure 6 we reported as an example the precipitation map of the month of March (top-right map) and a map reporting the sign of L in March (bottom-right map). The latter shows the areas for which the dry season has already started in March ($L < 0$, red areas) and those which are still in the wet season ($L \geq 0$, blue areas).

Particularly referring to the arable lands, which are the main part of the district, according to the collected information we simulated the cultivation of spring varieties in the non-irrigated land and the cultivation of summer ones in the irrigated land. Spring varieties are therefore more active in March than summer ones and this results in greater maximum evapotranspiration in the South-Western part of the district, even if the temperature is a little smaller.

As a term of comparison, the monthly maximum required evapotranspiration was calculated also as potential evapotranspiration with Thornthwaite's method, as proposed by the original Benfratello's paper. Data are not provided here for the sake of brevity but the effect of this scenario on the deficit estimate will be reported in the Discussion section.

5. RESULTS AND DISCUSSION

In Figure 7, the main components of the dimensionless water balance (α_{max}, α_{min}, δ) and the dimensionless uncertainty of the irrigation deficit $\sigma(\delta)$ are presented for the 1990 version of the land-cover map.

Despite α_{max} values being quite great, many areas of the district do not reach the field capacity ($\alpha_{max} = 1$) at the end of the wet season and most of the district would spontaneously reach very small water content values ($\alpha_{min} < 0.1$) at the end of the dry season, if not irrigated. Comparing Figure 7 with the field capacity reported in Figure 5 we recognize that the area most prone to reach the smallest α_{min} values are those characterized by the smallest U. This behavior is reflected in the assessment

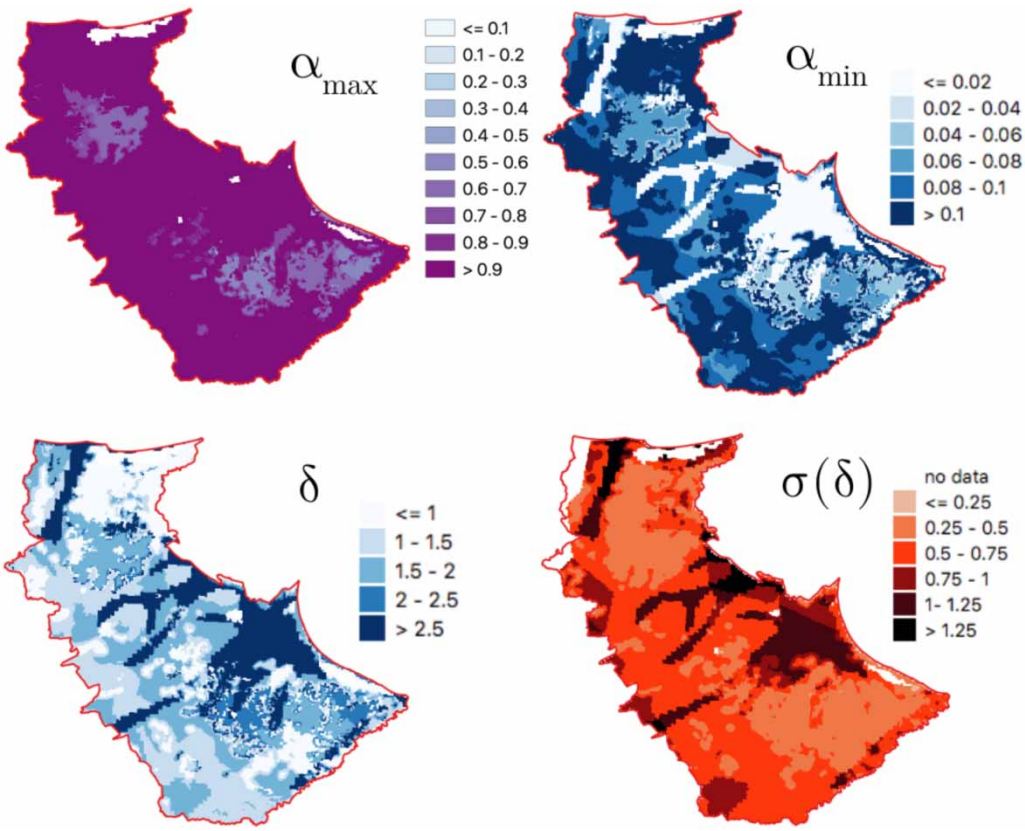

Figure 7 | Dimensionless components of Benfratello's water balance calculated for the land-cover classes of 1990. From top left to bottom right: maximum available soil water at the beginning of the dry season α_{max}, minimum available soil water at the end of the dry season α_{min}, expected annual deficit δ, uncertainty of the annual deficit $\sigma(\delta)$.

of the dimensionless irrigation deficit δ and of its uncertainty $\sigma(\delta)$, which results greatest where the field capacity U and α_{min} are smallest.

Figure 8 presents the expected annual irrigation deficit D and its uncertainty $\sigma(D)$ for the considered land-cover classes of 1990, 2000, 2006 and 2011. Comparing the four obtained spatial distributions of D, one sees how the areas characterized by higher values (i.e. $D > 600$ mm) have been decreasing since 1990, when they occupied the Northern and the South-Eastern parts of the district, to the point where they essentially disappeared in 2011. On the other hand, the central areas of the district experienced a first increase of D (from 200–300 to 300–400 mm and from 300–400 to 400–500 mm) from 1990 to 2006, followed by a decrease, as in 2011 there are just a few small areas with $D > 400$ mm. Recalling Figure 5 it is possible to relate the decrease in the width of the areas characterized by higher D values with a reduction in field capacity U in the Northern and South-Eastern parts of the district between 1990 and 2006, due mainly to an extensive change in cultivations typology, while there are no significant changes in U in the central part of the district despite some minor land-cover changes. If we consider the expected annual irrigation deficit uncertainty $\sigma(D)$ instead, Figure 8 depicts a situation which is essentially stationary between 1990 and 2011 and which appears to be greatly influenced by the precipitation dynamics. Indeed it shows spatial patterns that are very similar to those of the Thiessen–Voronoi tessellation applied for interpolating the precipitation data as reported in Figure 6 (top-right map).

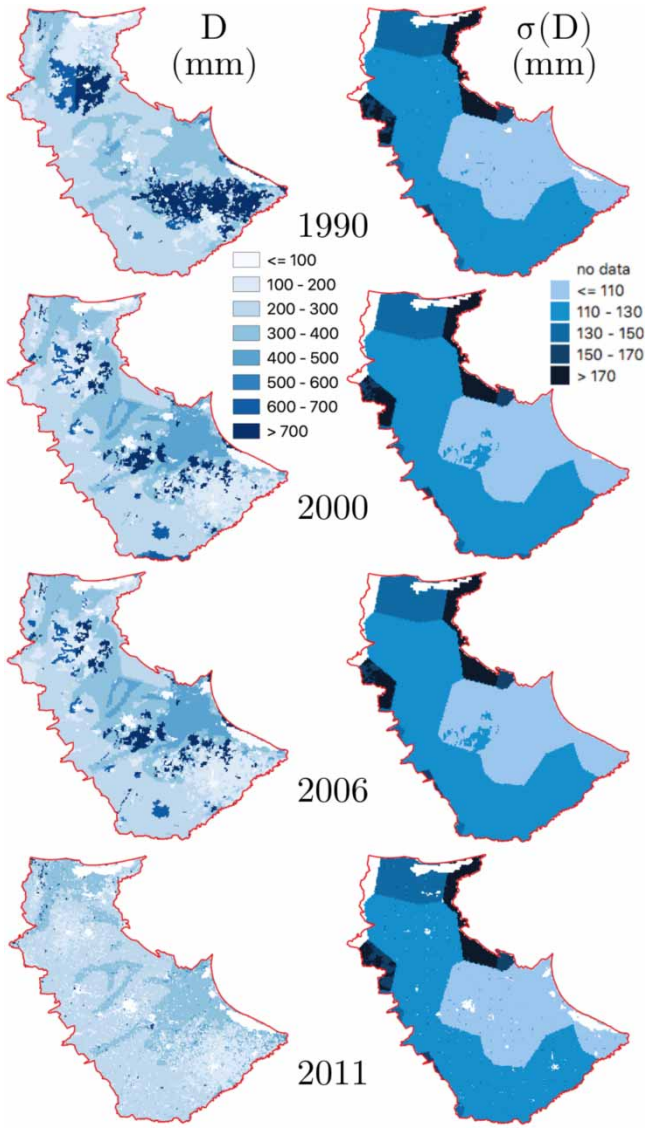

Figure 8 | Expected annual irrigation deficit D and its uncertainty $\sigma(D)$ for the land-cover classes of 1990, 2000, 2006 and 2011.

In Figure 9, we plot the distributions of crop-specific annual deficit values obtained by applying Benfratello's method in six different scenarios deriving from the combination of three different methods to assess the maximum required evapotranspiration (i.e. Hargreaves' method plus cultural coefficient, Hargreaves' method with no cultural coefficient and Thornwhaite's method) and two land-cover conditions (1990 and 2006).

The violin plots visualize the distribution densities while the white boxplots inside provide summary statistics (i.e. 25%, median and 75% quartiles). For the same maximum required evapotranspiration method, land-cover changes impact on the distribution densities but often do not affect the statistical summary in a meaningful way. Regarding the maximum required evapotranspiration methods, the cultural coefficients k_c bring the deficit values from Hargreaves' method closer to the ones from Thornwhaite's method for all the land-use classes except complex cultivation patterns.

In the figure, these results are also compared with both the average irrigation demands reported by Lamaddalena *et al.* (2004) and the erogated water volume ranges publicly stated by the authority managing the Capitanata reclamation and irrigation district, plotted with red dashed-dotted lines and black dashed lines, respectively (for the orchards land-use class the consortium provides only the maximum value of the erogated water). As it was not possible to provide a direct validation of the method in terms of comparison between a simulated and a measured sample of actual evapotranspiration data all over the Capitanata region, we propose a comparison between the average irrigation deficit values derived by the presented method (equal to 347 and 323 mm in 1990 and 2006, respectively) and the value estimated by Lamaddalena *et al.* (2004) for almost the same land-use classes (equal to 326 mm). By this comparison, we obtained a fair agreement, with an error of 6.4 and −1.1% if 1990 and 2006 land-use are considered, respectively. The results are also summarized in Table 4, where the ratio between the calculated deficit and the mean water supply provided by the consortium is reported. Apart from the cases of complex cultivation patterns and orchards, which are in many cases complex mosaic crops and would therefore require deeper insight into the actual cultivations, the estimated deficit is always smaller than the erogated water supply. Moreover, by comparing the average irrigation deficit with the recommended water volumes given by the Consortium, values of global irrigation efficiency of 82 and 92% are obtained for 1990 and 2006 land-use, respectively. These values are consistent with the drip- and micro-irrigation practices that are commonly and widely adopted in the Capitanata irrigation district.

In order to highlight the influence of the precipitation dynamics on the expected annual irrigation deficit uncertainty $\sigma(D)$, Figure 10 presents a plot of the $(\sigma(P), \sigma(D))$ pairs of every cell within the Capitanata territory for the considered land-cover classes of 1990, 2000, 2006 and 2011, for a total of 266,359 records. Despite some values laying outside from the scatter line, the sample – due to the great number of values – is well fitted by a linear model with equation:

$$\sigma(D) = 3.627 + 0.986\sigma(P), \quad R^2 = 0.9807, \tag{51}$$

with $\sigma(D)$ and $\sigma(P)$ in (mm). This means that despite the different land-cover classes (and the consequently different evapotranspirative demand and hydrological behavior) the irrigation deficit uncertainty is practically given by the interannual variability of the annual precipitation.

In Figure 11, we present the classical Budyko curve and the irrigation-deficit curve derived by it with the average annual water balance, for each cell and for each land-cover scenario.

The calculated water balances of the four scenarios are quite different from each other according to the scenarios of land-cover depicted by the Regional Authority. In fact, the 1990 and 2011 land-cover maps split many arable land areas between irrigated and non-irrigated, whereas the 2000 and 2006 maps classify all the arable lands as just non-irrigated. According to the collected information, the non-irrigated land is mainly cultivated with spring varieties whereas the irrigated land is mainly cultivated with summer varieties, and we maintained this set up in all the scenarios in order to appreciate how the land-cover change could have affected the general behavior of the district water balance. As the precipitation regime is typically Mediterranean, with a winter rainy season (Figure 3), the spring varieties can benefit from the water stored in the soil at the end of the rainy season. On the contrary, the summer varieties benefit less from the water stored in the soil during the rainy season. As a consequence, the clouds of the water balances for the 2000 and 2006 scenarios are more compact and nearer to the limit curves than those of the 1990 and 2011 scenarios, that are more spread and far from the limit curves. This results in greater estimates of the irrigation deficit for the 1990 and 2011 scenarios with respect to the 2000 and 2006 ones.

These findings are clearly represented in Figure 12, which reports a detail of the Budyko curve and of the irrigation-deficit curve only for the 1990 land-cover scenario, with evidence of the different land-cover classes. Almost all the classes, with the

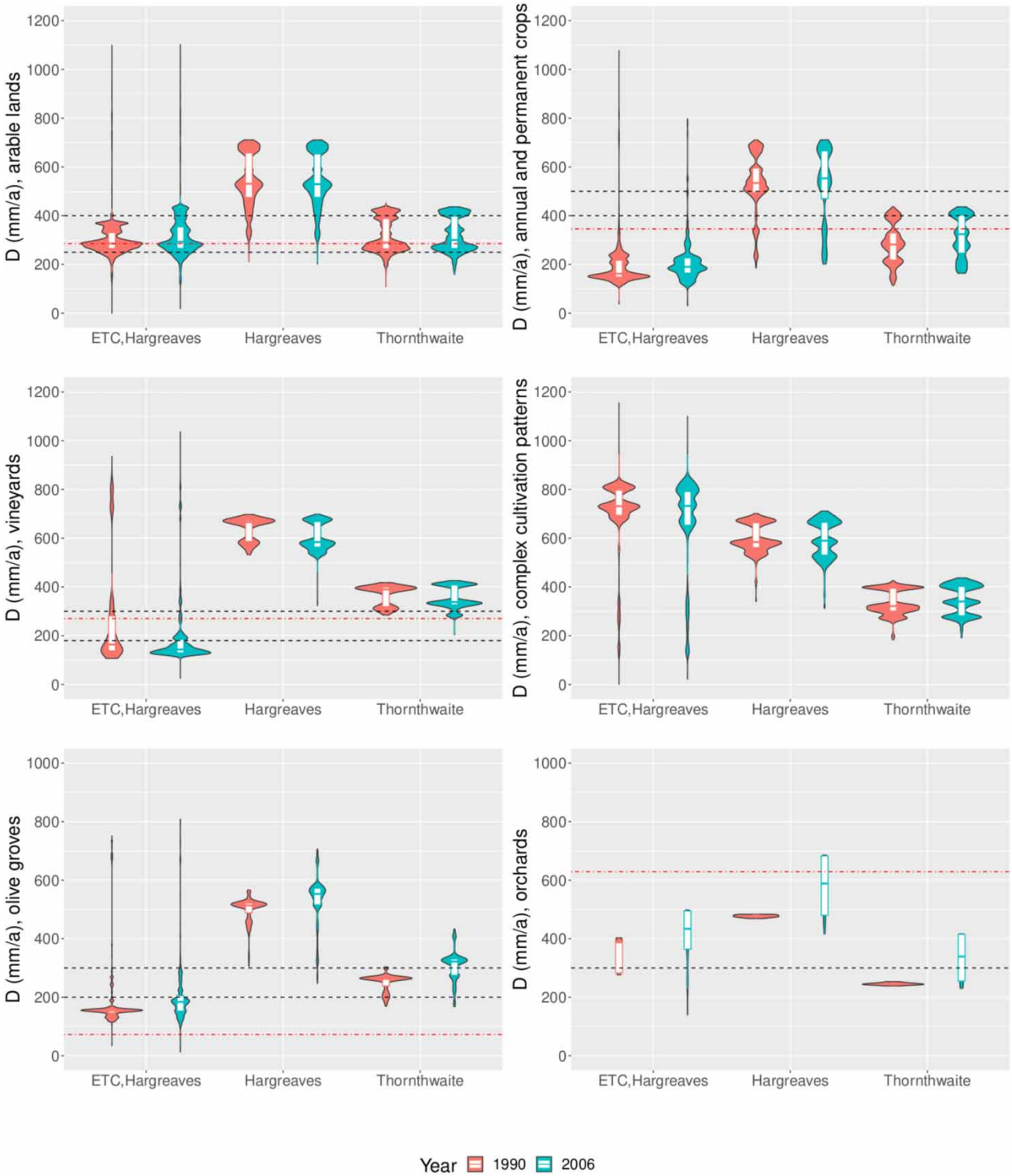

Figure 9 | Crop–specific annual deficit values obtained applying Benfratello's method in three different maximum evapotranspiration scenarios: violin plots visualize the distributions densities while the white boxplots provide summary statistics (25% median and 75% quartiles). Red dashed-dotted lines represent the average irrigation demands reported by Lamaddalena *et al.* (2004). Black dashed lines represent the ranges of crop-water requirements provided by the Capitanata reclamation and irrigation district authority (for the orchards land-use class the consortium provides only the maximum value of the erogated water). Please refer to the online version of this paper to see this figure in colour: http://dx.doi.org/10.2166/nh.2023.081.

Table 4 | Summary data of the calculated irrigation deficits for 1990 and 2006 land-use scenarios

	WS			1990 land-use					2006 land-use				
Land-use class	Max (mm)	Min (mm)	Mean (mm)	Area %	Med(*D*) (mm)	⟨*D*⟩ (mm)	⟨σ(*D*)⟩ (mm)	⟨*D*⟩/⟨*WS*⟩ (mm/mm)	Area %	Med(*D*) (mm)	⟨*D*⟩ (mm)	⟨σ(*D*)⟩ (mm)	⟨*D*⟩/⟨*WS*⟩ (mm/mm)
Arable lands	400	250	325	64.88	286	299		0.92	68.26	293	315		0.97
Annual cr.	500	400	450	12.63	162	192		0.43	3.31	190	206		0.46
Vineyards	300	180	240	1.26	164	269		1.12	9.32	144	184		0.77
Complex patt.				15.26	731	700			8.01	732	665		
Olive groves	300	200	250	1.25	154	183		0.73	4.53	184	198		0.79
Orchards			300	0.03	388	353		1.18	0.21	434	409		1.36
Other				4.71					6.35				
Capitanata				100	287	347	122	0.82	100	287	323	122	0.92

Note: WS, water supply provided by the Capitanata consortium; Area, percentual coverage of each land-use class; Med(*D*), (Spatial) median value of the calculated deficit *D*; ⟨*D*⟩, Spatial average of *D*; ⟨σ(D)⟩, spatial average of the uncertainty $\sigma(D)$. Abbreviated land-use classes are as follows: Annual cr., Annual and permanent crops; Complex patt., Complex cultivation patterns.

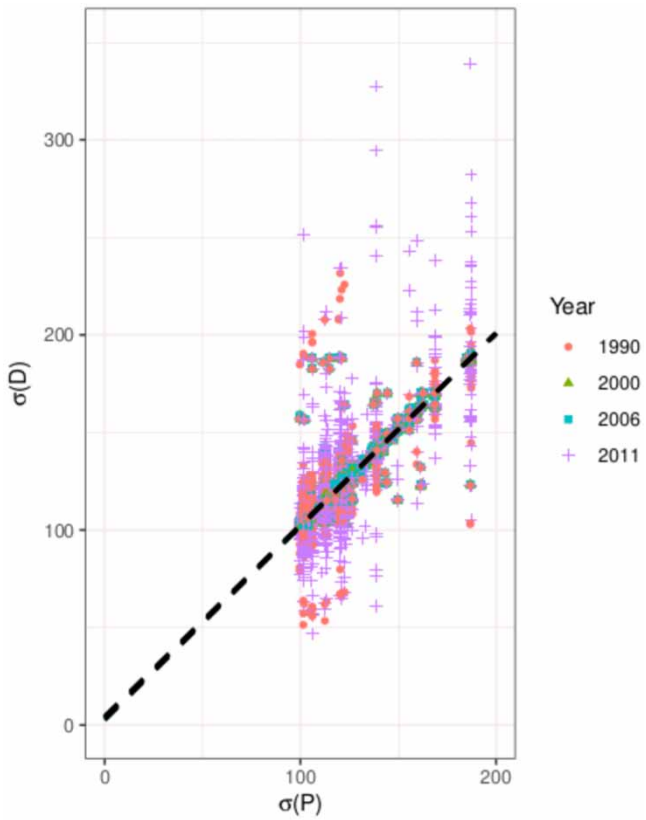

Figure 10 | Influence of the precipitation interannual variability $\sigma(P)$ on the expected annual irrigation deficit uncertainty $\sigma(D)$: $\sigma(D) = 3.627 + 0.986\sigma(P)$, $R^2 = 0.9807$.

exception of the irrigated arable land, lay either along the Budyko curve or between the Budyko curve and the limit curve. The irrigated arable land, instead, is spontaneously characterized by a small evapotranspiration and lays under the Budyko curve, consequently needing a greater irrigation demand, with respect to that compatible with the Budyko curve.

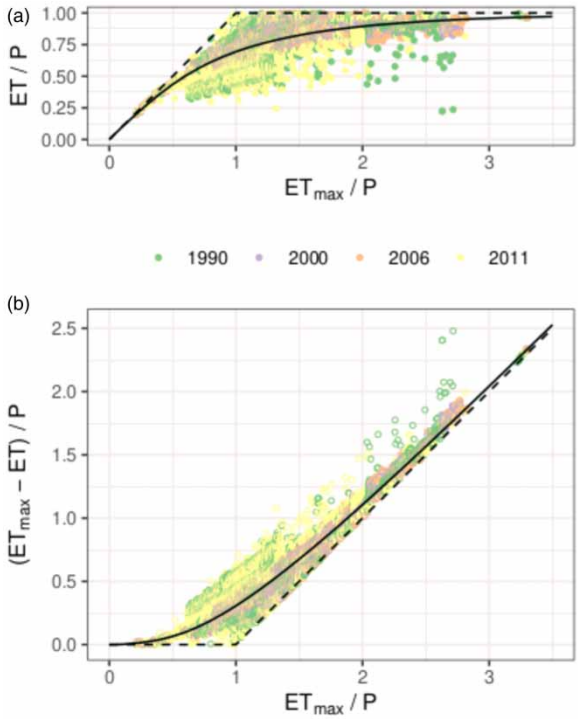

Figure 11 | (a) Budyko curve and calculated water balance components for each cell of the Capitanata district in the 1990, 2000, 2006, 2011 scenarios of land-cover classification. (b) Irrigation-deficit curves based on the Budyko curve and on its limit curve, and calculated irrigation deficits for each cell of the Capitanata district in the aforementioned land-cover classification scenarios.

6. CONCLUSIONS

Our aim was to provide a robust and easy-to-use tool that allows us to make distributed estimates of irrigation deficits at the district level, in order to estimate the expected variations of the deficit in both climate and anthropogenic change scenarios. For this purpose we have proposed a GIS-based implementation of Benfratello's method, which allows us to estimate the deficit as a climatic characteristic on the basis of the knowledge of the precipitation regimes, the maximum required evapotranspiration and of the soil field capacity. The presented model couples the solidity of the results with a low computational burden, and could work as a webGIS tool for water management and irrigation advisory. The method was originally designed for Mediterranean semiarid climates and it is suitable for all semiarid climates. In order to extend its potential, we have also defined relationships that allow estimation of the deficit uncertainty. The model was applied to the case study of Capitanata agricultural district, for which the reference climate was defined on the basis of data collected at 19 stations with data series lengths ranging from 15 to 62 years. In compliance with the original simplicity of the method, the maps of the precipitation and temperature regimes were obtained with the Thiessen–Voronoi tessellation and with an altitudinal gradient, respectively, and the maximum required evapotranspiration was determined both with Thornthwaite's method and Hargreaves' method, modulated with the FAO procedure proposed by Allen *et al.* (1998). However, the method is flexible and its application is independent of how the input maps are generated. Simulations were carried out in four different land-use scenarios available for the case study area, with reference to the years 1990, 2000, 2006 and 2011. The estimated irrigation deficit, summarized in Table 4 for different land-use classes, was compared with both the values reported by Lamaddalena *et al.* (2004) and the irrigation supply declared by the Consortium, obtaining an overall good agreement: the first comparison produced an error of 6.4 and −1.1% if 1990 and 2006 land-use were considered, respectively, while the second one obtained values of global irrigation efficiency of 82 and 92% (for 1990 and 2006 land-use, respectively), consistent with the drip- and micro-irrigation practices that are commonly and widely adopted in the Capitanata irrigation district. Uncertainty maps were produced and it was observed how the deficit uncertainty is practically attributable to the precipitation interannual variability, while the effects of the interannual variability of the evapotranspiration demand – resulting from the temperature variability according to the applied model – are minimal. The results were then represented on a Budyko curve and on a deficit curve (as

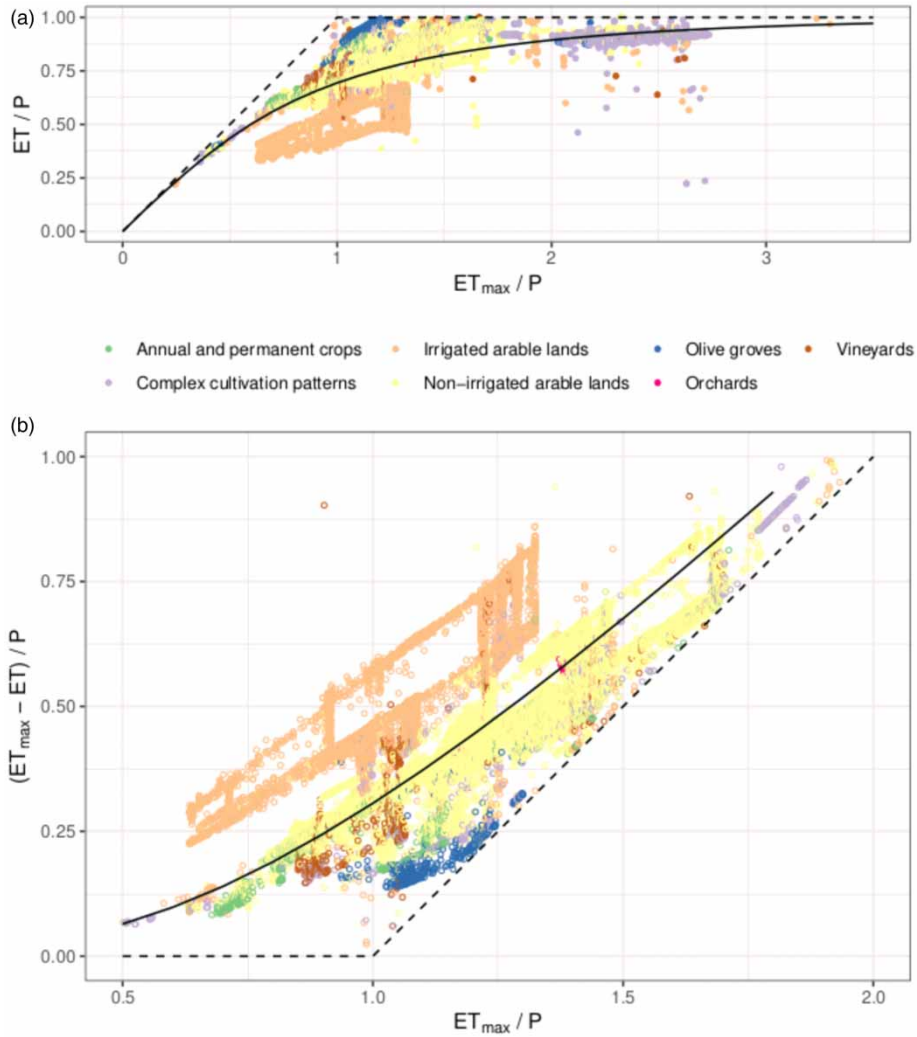

Figure 12 | (a) Budyko curve and calculated water balance components for each cell of the Capitanata district in the 1990 land-cover scenario, clustered for the land-cover classes. (b) Irrigation-deficit curves based on the Budyko curve and on its limit curve, and calculated irrigation deficits for the 1990 land-cover scenario, clustered for the land-cover classes (zoom on the range $0.5 < ET_{max}/P < 2$).

a function of the aridity index) derived from the Budyko curve. It was thus observed that most of the crops (apart from the crops grown on irrigated arable land) are well identified by the area between the Budyko curve and the limit curves, the latter of which corresponds to the minimization of the irrigation deficit. The case is instead different for the irrigated arable land which, being able to benefit from irrigation, deviates from the natural hydrological behavior of the soil, thus showing a greater irrigation demand. It is our main conclusion that, due to its simplicity and the small number of needed parameters, Benfratello's method (although developed in the 1960s) might still be regarded as an effective tool to assess the effects of climatic, land-use and anthropogenic change scenarios on the soil water balance and on the irrigation deficit.

ACKNOWLEDGEMENTS

This study was supported by the project *SWaRM–Net Smart Water Resource Management Networks*[2], by the Water Research Institute (IRSA) of the Italian National Research Council (CNR) and by the University of Brescia. We greatfully thank the Centro Funzionale Decentrato of the Apulia Region for providing the data, and Dr Emanuele Romano (CNR–IRSA). This

[2] https://www.cnr.it/it/progetti-di-ricerca/progetto/39395/swarm-net-dta-ad002-554

paper is dedicated to the memory of our friend and colleague Prof. Giuseppe Provenzano, who passed away in December 2022. He was part of the School of Agricultural Hydrology in Palermo, founded by Guglielmo Benfratello, and when we started to deal with Benfratello's water balance method he gave us inspiring and encouraging suggestions to develop our research.

DATA AVAILABILITY STATEMENT

Data cannot be made publicly available; readers should contact the corresponding author for details.

CONFLICT OF INTEREST

The authors declare there is no conflict.

REFERENCES

Allen, R. G., Pereira, L. S., Raes, D. & Smith, M. 1998 Crop evapotranspiration guidelines for computing crop water requirements-FAO irrigation and drainage paper 56. *FAO, Rome* **300** (9), D05109.

Ancona, V., Bruno, D. E., Lopez, N., Pappagallo, G. & Uricchio, V. F. 2010 A Modified Soil Quality Index to Assess the Influence of Soil Degradation Processes on Desertification Risk: The Apulia Case. *Italian Journal of Agronomy* **5** (53), 45–56.

Arias, P., Bellouin, N., Coppola, E., Jones, R., Krinner, G., Marotzke, J., Naik, V., Palmer, M., Plattner, G.-K., Rogelj, J., Rojas, M., Sillmann, J., Storelvmo, T., Thorne, P., Trewin, B., Rao, K. A., Adhikary, B., Allan, R., Armour, K., Bala, G., Barimalala, R., Berger, S., Canadell, J., Cassou, C., Cherchi, A., Collins, W., Collins, W., Connors, S., Corti, S., Cruz, F., Dentener, F., Dereczynski, C., Luca, A. D., Niang, A. D., Doblas-Reyes, F., Dosio, A., Douville, H., Engelbrecht, F., Eyring, V., Fischer, E., Forster, P., Fox-Kemper, B., Fuglestvedt, J., Fyfe, J., Gillett, N., Goldfarb, L., Gorodetskaya, I., Gutierrez, J., Hamdi, R., Hawkins, E., Hewitt, H., Hope, P., Islam, A., Jones, C., Kaufman, D., Kopp, R., Kosaka, Y., Kossin, J., Krakovska, S., Lee, J.-Y., Li, J., Mauritsen, T., Maycock, T., Meinshausen, M., Min, S.-K., Monteiro, P., Ngo-Duc, T., Otto, F., Pinto, I., Pirani, A., Raghavan, K., Ranasinghe, R., Ruane, A., Ruiz, L., Sallée, J.-B., Samset, B., Sathyendranath, S., Seneviratne, S., Sörensson, A., Szopa, S., Takayabu, I., Tréguier, A.-M., van den Hurk, B., Vautard, R., von Schuckmann, K., Zaehle, S., Zhang, X. & Zickfeld, K. 2021 Technical summary. In: Masson-Delmotte V., Zhai P. , Pirani A., Connors S. L., Péan C., Berger S., Caud N., Chen Y., Goldfarb L., Gomis M. I., Huang M., Leitzell K., Lonnoy E., Matthews J. B. R., Maycock T. K., Waterfield T., Yelekçi O., Yu R. & Zhou B. (eds). *Climate Change 2021: The Physical Science Basis. Contribution of Working Group I to the Sixth Assessment Report of the Intergovernmental Panel on Climate Change*. Cambridge University Press, Cambridge, United Kingdom; New York, NY, USA, pp. 33–144.

Baltas, E. 2007 Spatial distribution of climatic indices in northern Greece. *Meteorological Applications* **14** (1), 69–78. Available from: https://rmets.onlinelibrary.wiley.com/doi/abs/10.1002/met.7

Bandini, A. 1931 Tipi pluviometrici dominanti sulle regioni italiane. In: *Il Servizio Idrografico Italiano. XV Congresso Internazionale di Navigazione*. Min LL. PP., Regno d'Italia, Tipografia del Senato, Roma, pp. 111–118.

Bartolini, E., Allamano, P., Laio, F. & Claps, P. 2011 Runoff regime estimation at high-elevation sites: a parsimonious water balance approach. *Hydrology and Earth System Sciences* **15** (5), 1661–1673. Available from: https://hess.copernicus.org/articles/15/1661/2011/

Benfratello, G. 1961 Contributo allo studio del bilancio idrologico del terreno agrario. *L'Acqua* (2), 34–53.

Benfratello, G. 1964 Programmazione di un computo di idrologia su calcolatrice elettronica numerica. In: *Atti della Accademia di Scienze, Lettere e Arti di Palermo, Serie IV, Vol. XXIII, Parte I, Anno Accademico 1962–1963*. Accademia di Scienze, Lettere e Arti di Palermo, Palermo, Italy, pp. 197–235.

Benfratello, G., Melisenda Giambertoni, I. & Santoro, M. 1979 Hydrogeological research aimed at the exploitation of aquifers in some areas in sicily. In: *Proceedings of the 18th IAHR World Congress 'Hydraulic Engineering in Water Resources Development and Management', vol. 5: Subject D – Physical and Mathematical Models for Watersheds*. IAHR, Cagliari, pp. 135–143.

Braca, G., Bussettini, M., Ducci, D., Lastoria, B. & Mariani, S. 2019 Evaluation of national and regional groundwater resources under climate change scenarios using a Gis-based water budget procedure. *Rendiconti Lincei. Scienze Fisiche E Naturali* **30** (1), 109–123. https://doi.org/10.1007/s12210-018-00757-6.

Braca, G., Bussettini, M., Lastoria, B., Mariani, S. & Piva, F. 2021 *Il Bilancio Idrologico Gis Based a scala Nazionale su Griglia regolare – BIGBANG: metodologia e stime. Rapporto sulla disponibilità naturale della risorsa idrica*. Rapporto 339/21, Istituto Superiore per la Protezione e la Ricerca Ambientale, Roma.

Brussolo, E., Palazzi, E., von Hardenberg, J., Masetti, G., Vivaldo, G., Previati, M., Canone, D., Gisolo, D., Bevilacqua, I., Provenzale, A. & Ferraris, S. 2022 Aquifer recharge in the Piedmont Alpine zone: historical trends and future scenarios. *Hydrology and Earth System Sciences* **26** (2), 407–427. Available from: https://hess.copernicus.org/articles/26/407/2022/

Budyko, M. I. 1974 *Climate and Life. No. Vol. 18 in International Geophysics Series*. Academic Press. Available from: https://proxy.unibs.it/login?url=https://search.ebscohost.com/login.aspx?direct=true&db=nlebk&AN=297011&lang=it&site=eds-live&scope=site

Casadei, S., Mannocchi, F., Mecarelli, P., 1993 Operational hydrology and reservoir management in the upper tiber river basin. In: *Extreme Hydrological Events: Precipitation, Floods and Droughts, no. 213 in IAHS Publications* (Kundzewicz, Z., Rosbjerg, D., Simonovic, S. & Takeuchi, K., eds). Int Assoc Hydrol Sci; Int Assoc Meteorol & Atmospher Phys; UNESCO, Int Assoc Hydrological Sciences. International Symposium on Extreme Hydrological Events: Precipitation, Floods and Droughts, Yokohama, Japan, Jul 20–23, 1993, pp. 393–402.

Chen, D., Shams, S., Carmona-Moreno, C. & Leone, A. 2010 Assessment of open source GIS software for water resources management in developing countries. *Journal of Hydro-Environment Research* **4** (3), 253–264. Available from: https://www.sciencedirect.com/science/article/pii/S1570644310000511

da Silva Tavares, P., Giarolla, A., Chou, S. C., de Paula Silva, A. J. & de Arruda Lyra, A. 2018 Climate change impact on the potential yield of Arabica coffee in southeast Brazil. *Regional Environmental Change* **18** (3), 873–883.

De Varennes e Mendonça, P. 1958 Sobre o novo método de balanço hidrológico do solo de Thornthwaite-Mather. *Anais do Instituto Superior de Agronomia* **22**, 271.

de Vito, R., Pagano, A., Portoghese, I., Giordano, R., Vurro, M. & Fratino, U. 2019 Integrated Approach for Supporting Sustainable Water Resources Management of Irrigation Based on the WEFN Framework. *Water Resources Management* **33** (4), 1281–1295.

Dourado-Neto, D., van Lier, J., d, Q., Metselaar, K., Reichardt, K. & Nielsen, D. R. 2010 General procedure to initialize the cyclic soil water balance by the Thornthwaite and Mather method. *Scientia Agricola* **67**, 87–95.

Dragonetti, G., Sengouga, A., Comegna, A., Lamaddalena, N., Basile, A., Coppola, A. 2020 SIRR-MOD—A Decision Support System for Identifying Optimal Irrigation Water Needs at Field and District Scale. In: *MID-TERM AIIA 2019: Innovative Biosystems Engineering for Sustainable Agriculture, Forestry and Food Production, vol. 67 of Lecture Notes in Civil Engineering* (Coppola, A., Di Renzo, G. C., Altieri, G. & D'Antonio, P., eds). Springer International Publishing, Cham, pp. 117–124.

Dumitru, S., Chendes, V., Cojocaru, G. & Simota, C. 2009 Developing an integrated crop-meteorological model for hilly terrains using digital terrain models. *Scientific Papers. Series A* **LII**, 147–152.

D'Urso, G., Menenti, M. & Santini, A. 1999 Regional application of one-dimensional water flow models for irrigation management. *Agricultural Water Management* **40** (2-3), 291–302.

FAO 2021 *Tracking Progress on Food and Agriculture-Related SDG Indicators 2021: A Report on the Indicators Under FAO Custodianship*. FAO, Rome. https://doi.org/10.4060/cb6872en.

Farthing, M. W. & Ogden, F. L. 2017 Numerical solution of Richards' equation: a review of advances and challenges. *Soil Science Society of America Journal* **81** (6), 1257–1269. Available from: https://acsess.onlinelibrary.wiley.com/doi/abs/10.2136/sssaj2017.02.0058

Foxx, T. S., Tierney, G. D. & Williams, J. M. 1984 *Rooting Depths of Plants Relative to Biological and Environmental Factors*. Tech. rep., Los Alamos National Lab., NM, USA.

Guyennon, N., Romano, E. & Portoghese, I. 2016 Long-term climate sensitivity of an integrated water supply system: the role of irrigation. *Science of The Total Environment* **565**, 68–81. Available from: https://www.sciencedirect.com/science/article/pii/S0048969716308518

Guyennon, N., Salerno, F., Portoghese, I. & Romano, E. 2017 Climate change adaptation in a Mediterranean semi-arid catchment: testing managed aquifer recharge and increased surface reservoir capacity. *Water* **9** (9). Available from: https://www.mdpi.com/2073-4441/9/9/689

Lamaddalena, N., Hamdy, A., Todorovic, M. & Quarto, A. 2004 Participatory water management in Italy: Case study of the Consortium Bonifica della Capitanata. *Options Mediterranennes Series B* **48**, 159–169.

Lamaddalena, N., Caliandro, A., Daccache, A., D'Agostino, D., Scardigno, A. & De Santis, S. 2008 Riorientamenti produttivi del territorio agricolo pugliese per uno sviluppo rurale sostenibile. *Regione Puglia and CIHEAM-IAMB*, 93pp.

Licciardello, F., Rossi, C. G., Srinivasan, R., Zimbone, S. M. & Barbagallo, S. 2011 Hydrologic evaluation of a Mediterranean watershed using the SWAT model with multiple PET estimation methods. *Transactions of the ASABE* **54** (5), 1615–1625. https://doi.org/10.13031/2013.39840.

Mantica, I. 1975 Primi risultati di un'Indagine circa la correlazione tra afflussi e deflussi nei bacini abruzzesi con corso d'acqua con foce sul litorale adriatico. In: *Notizie dell'economia teramana: pubblicazione mensile della Camera di commercio, industria e agricoltura di Teramo*. C.E.T.I., Teramo, pp. 20–47.

Melisenda, I. 1964 Sui calcoli idrologici per il terreno agrario: influenza del 'clima'. *L'Acqua* (4), 3–20.

Melisenda, I. 1965 Sul calcolo dell'evapotraspirazione nell'ambiente siciliano. In: *Atti della Accademia di Scienze, Lettere e Arti di Palermo, Serie IV, Vol. XXIV, Parte I, Anno Accademico 1963–1964*. Accademia di Scienze, Lettere e Arti di Palermo, Palermo, Italy, pp. 291–328.

Melisenda, I. 1967a Possibilité de déduction des besoins en eau d'irrigation à partir de la loi de dessèchement du sol. *La Houille Blanche* **53** (8), 829–839.

Melisenda, I. 1967b Su una classificazione del clima basata sui parametri dell'idrologia agraria. In: *Atti della Accademia di Scienze, Lettere e Arti di Palermo, Serie IV, Vol. XXVI, Parte I, Anno Accademico 1965–1966*. Accademia di Scienze, Lettere e Arti di Palermo, Palermo, Italy, pp. 381–417.

Nistor, M.-M., Man, T. C., Benzaghta, M. A., Nedumpallile Vasu, N., Dezsi, Ş. & Kizza, R. 2018 Land cover and temperature implications for the seasonal evapotranspiration in Europe. *Geographia Technica* **13** (1), 85–108.

Peel, M. C., Finlayson, B. L. & McMahon, T. A. 2007 Updated world map of the Köppen-Geiger climate classification. *Hydrology and Earth System Sciences* **11** (5), 1633–1644. Available from: https://hess.copernicus.org/articles/11/1633/2007/

Pereira, L., Paredes, P. & Jovanovic, N. 2020 Soil water balance models for determining crop water and irrigation requirements and irrigation scheduling focusing on the FAO56 method and the dual kc approach. *Agricultural Water Management* **241**, 106357. Available from: https://www.sciencedirect.com/science/article/pii/S0378377420303930

Portoghese, I., Uricchio, V. & Vurro, M. 2005 A GIS tool for hydrogeological water balance evaluation on a regional scale in semi-arid environments. *Computers & Geosciences* **31** (1), 15–27. Available from: https://www.sciencedirect.com/science/article/pii/S009830040400144X

Quignones, R. 1974 Correlazione tra afflussi e deflussi dei principali bacini siciliani. *L'ingegnere* **49**, 243–265.

Romano, N. 2014 Soil moisture at local scale: measurements and simulations. *Journal of Hydrology* **516**, 6–20. Determination of soil moisture: Measurements and theoretical approaches. Available from: https://www.sciencedirect.com/science/article/pii/S0022169414000328

Santini, A. 1979 Water balance of the soil-plant system: the use of a mathematical simulation model. *Rivista di ingegneria agraria* **10** (2), 63–76.

Santini, A. 1992 Modelling water dynamics in the soil-plant-atmosphere system for irrigation problems. *Excerpta of the Italian Contributions to the Field of Hydraulic Engineering* **6**, 133–166.

Santoro, M. 1970 Sul calcolo numerico del bilancio idrologico del terreno agrario. In: *Atti della Accademia di Scienze, Lettere e Arti di Palermo, Serie IV, Vol. XXIX, Parte I, Anno Accademico 1968–1969*. Accademia di Scienze, Lettere e Arti di Palermo, Palermo, Italy, pp. 359–394.

Santoro, M. 1991 Il bilancio idrico del terreno agrario. In: Corso di Aggiornamento: Modelli Idrologici Superficiali nella Pianificazione di Bacino, 10-14 giugno 1991. Programma di Istruzione Permanente del Politecnico di Milano, CittàStudi, Milano, pp. 443–487.

Scalenghe, R. & Ferraris, S. 2009 The First Forty Years of a Technosol. *Pedosphere* **19** (1), 40–52. Available from: https://www.sciencedirect.com/science/article/pii/S100201600860082X

Thornthwaite, C. W. 1948 An approach toward a rational classification of climate. *Geographical Review* **38** (1), 55–94. Available from: http://www.jstor.org/stable/210739

Thornthwaite, C. & Mather, J. 1955a The Water Budget and Its Use in Irrigation. In: *The Yearbook of Agriculture 1955: Water*. U.S. Government Printing Office, Washington, DC, pp. 346–358.

Thornthwaite, C. W. & Mather, J. R 1955b The water balance. In: *Publications in Climatology*, **VIII** (1), Drexel Institute of Technology, Laboratory of Climatology, Centerton, New Jersey.

Thornthwaite, C. W. & Mather, J. R. 1957 Instructions and tables for computing potential evapotranspiration and the water balance. In: *Publications in Climatology*, **X** (3), Drexel Institute of Technology, Laboratory of Climatology, Centerton, New Jersey.

UN–Water 2022 *The United Nations World Water Development Report 2022: Groundwater: Making the Invisible Visible. The United Nations World Water Development Report*. United Nations Educational, Scientific and Cultural Organization, Paris, France.

Ventrella, D., Charfeddine, M., Moriondo, M., Rinaldi, M. & Bindi, M. 2012 Agronomic adaptation strategies under climate change for winter durum wheat and tomato in southern Italy: irrigation and nitrogen fertilization. *Regional Environmental Change* **12**, 407–419. https://doi.org/10.1007/s10113-011-0256-3.

Verma, S., Verma, R. K., Singh, A., Naik, N. S., 2012 Web-Based GIS and Desktop Open Source GIS Software: An Emerging Innovative Approach for Water Resources Management. In: *Advances in Computer Science, Engineering & Applications* (Wyld, D. C., Zizka, J. & Nagamalai, D., eds). Springer Berlin Heidelberg, Berlin, Heidelberg, pp. 1061–1074.

Viparelli, C. 1956a Bilanci idrologici di alcuni gruppi di bacini impermeabili dell'Italia meridionale e insulare. *L'Acqua*.

Viparelli, C. 1956b Possibilità di regolazione dei bacini impermeabili dell'Italia meridionale. *L'Acqua*.

Viparelli, R. & Versace, P. 1979 *Distribuzione di probabilità dei deflussi D. Tech. Rep. 421*. Università di Napoli, Istituti Idraulici.

Vitale, D., Rana, G. & Soldo, P. 2010 Trends and Extremes Analysis of Daily Weather Data from a Site in the Capitanata Plain (Southern Italy). *Italian Journal of Agronomy* **5** (2), 133–144.

Walker, W. 1989 *Guidelines for Designing and Evaluating Surface Irrigation Systems*. FAO, Rome.

Xu, C.-Y. & Singh, V. P. 1998 A Review on Monthly Water Balance Models for Water Resources Investigations. *Water Resources Management* **12** (1), 20–50. https://doi.org/10.1023/A:1007916816469.

First received 30 July 2022; accepted in revised form 21 February 2023. Available online 10 March 2023